CERN LIBRARIES, GENEVA

CM-P00060452

Archives

Ref.TH.1700-CERN

MULTIPLICITY DISTRIBUTIONS AND INCLUSIVE SPECTRA IN A MULTIPERIPHERAL CLUSTER EMISSION MODEL

E.L. Berger
CERN - Geneva

and

G. C. Fox
CALTECH - Pasadena

A B S T R A C T

A simple two-parameter model incorporating pion clusters produced with a multiperipheral-like matrix element is proposed. It gives a good qualitative description of multiplicity, and of single- and two-particle rapidity distributions above 50 GeV/c.

Ref.TH.1700-CERN
6 July 1973

Hadronic multiparticle production data at high energy show important evidence for diffractive effects, for cluster formation, and for short-range order characteristic of multiperipheral-type models. The apparently scaling leading proton peak [1] is a striking signal of inelastic diffraction. Dominance of short-range order effects in the central region is suggested by the plateau in rapidity for single-pion inclusive spectra [2] and, more importantly, by the energy independence of normalized two-particle inclusive correlations [3],[4]. Cluster formation seems evident. Small average spacing in rapidity and a mean two-pion invariant mass of $\lesssim 500$ MeV are consequences of relatively large values observed [5] for $\langle n_{ch} \rangle$. Clustering is called for more directly by the positive value of correlation moment f_2 for $p_{lab} \gtrsim 50$ GeV/c in pp collisions [5]. All three ingredients should be present in a realistic treatment of inclusive spectra and multiplicity distributions.

Until now, phenomenological approaches have concentrated on only a subset of the three items mentioned above. In the nova picture [6], cluster formation and diffraction are (over) emphasized, with result that correlations in the central region are predicted to be too large at ISR energies and to grow in proportion to $\sqrt{s}$. Independent pion emission models [7] are unable to produce the observed positive correlations. Two-component models for multiplicity distributions [8] have enjoyed great popularity. In this approach, positive f_2 and positive central region correlations arise simply from the addition of distributions. However, separation into components and the parametrization of each component is rather arbitrary. There is little predictive power. Inclusive Regge (Mueller) analysis [9] provides important insight, but fails to give reliable estimates of the scale of energy dependent effects, especially where "thresholds" are involved. Further, it is clearly unappropriate when non-inclusive aspects of multiparticle phenomena must be confronted.

In this note, we report results based on a model which combines the three ideas listed above. The approach is basically multiperipheral (short-range order dominated), with hadronic clusters rather than single hadrons being emitted along the multiperipheral chain. Diffractive effects are effectively taken into account by an amplitude in which Pomeron exchange is present. At least qualitative agreement is achieved with data on multiplicity distributions and on single and two-particle inclusive distributions.

We first define the model and then discuss its predictions using both a Monte Carlo phase space calculation and analytic evaluation of idealized limits.

1. THE MODEL AND ITS PARAMETERS

a) Multiperipheral cluster model

Figure 1a illustrates the production of clusters, each decaying into K particles by the exchange of some trajectory (e.g., π exchange). A very simple realization of this is given by an independent emission model in which the matrix element M for the emission of n_c clusters is given for $n_c \geq 2$ by

$$|M|^2 \propto \frac{\lambda^{n_c}}{n_c!} \prod_{i=1}^{n_c} \exp\left[-p_T^2|_i / 2\sigma_1^2\right] \qquad (1)$$

Following Hamer [10),11)], we suppose that the clusters are described by the statistical bootstrap theory [12)] and each decays isotropically in its rest frame into pions with distribution

$$D_\pi(p^2) \propto \exp\left[-p^2/2\sigma_2^2\right] \qquad (2)$$

This implies a linear relation between the mass m_c and the number of decay particles K of the cluster

$$m_c \approx 1.6\,\sigma_2 K \qquad (3)$$

K is not expected to be fixed. The clusters are surely produced with some mass spectrum. The results discussed in the paper are not sensitive to this, and and so we assume K is distributed uniformly between 1 and K_{max}, where K_{max} is energy independent and will be varied to fit the data.

We note that Hamer and Peierls [11)] have given a theoretical analysis of a multiperipheral cluster model which, for π exchange, has a similar matrix element to (1). In fact, it is encouraging that they find an output trajectory (Pomeron) near $\alpha = 1$ for parameters similar to those we find from our fit to data [see our Eq. (9) later].

b) Final state baryons

In principle, one could calculate the whole final state using a model, as sketched in a), where the clusters decay into pions, protons and all the other stable hadrons. However, this would require many different exchanges in our multiperipheral links and a very detailed specification of their quantum numbers. Rather, we first simplify to a world containing only pions and nucleons,

and then use as input to the model the observed nucleon momentum distribution. After we feed in the known proton-neutron ratio and the confinement of baryons to small p_T^2, crucial input is the inclusive proton $d\sigma/dx$ distribution. Given this, and assuming that the two final state baryons are produced independently, we derive a definite distribution for the invariant mass m_B of the remaining pion system. It is to this system that we apply the simple model described in a) for every m_B to predict the pion multiplicities and single and two-particle inclusive distributions.

Our parameters can be classified as follows : λ [in Eq. (1)] and K_{max} are free and determined from observed multiplicity distributions (Section 2.a) $d\sigma/dx|_{proton}$ and σ_2 are roughly known but have some 20% freedom (Sections 1.c and 2.b); the results are insensitive to σ_1 (Section 2.b).

c) x spectrum for protons

We can divide the contributions to $d\sigma/dx$ into the two parts sketched in Figs. 1b and 1c corresponding to Pomeron and P' contributions. We choose the currently fashionable [13] model with a non-vanishing triple Pomeron coupling in which Fig. 1b is represented as

$$E\frac{d\sigma}{d^3p} \equiv f(s,x,p_T^2) \sim B/(1-x) \qquad (4)$$

As has been recently pointed out by several authors [13], the rise in the total cross-section at ISR energies can be attributed to this term. We choose a magnitude B consistent with this interpretation. All other contributions to $d\sigma/dx$ are assigned to graph 1c, but we need no detailed triple Regge model. Rather we take this x distribution from experiment [1] as adding to (4) a smooth function of x which we choose to have $\langle|x|\rangle = 0.45$. Values between $\langle|x|\rangle = 0.4$ to 0.5 allow similar fits with 10% changes in parameters. For analytic estimates, we use the rough parametrization

$$f(x) = A + B/(1-x) \qquad (5)$$
$$\text{with } A/B \approx 40$$

We note that the two terms in (5) give this picture many of the features of the "two-component" approach [8]. However, the quantitative results are changed because the Pomeron contribution is not a single added term, but rather an integral which diverges near $x = 1$. In particular, the Pomeron is associated with a logarithmically growing multiplicity, in contrast to the fixed multiplicity of many two-component models. The growing multiplicity appears to be inevitable for a Pomeron associated with a scaling (in x) peak in $f(x,p_T^2)$ near $x = 1$. As we will point out in the next Section, there are other important differences for f_2, and both single and two-particle rapidity distributions.

d) Treatment of charges

In principle one should perhaps assign definite probabilities for isospins of the exchanged links and produced cluster. Unfortunately, the necessary analysis in the statistical bootstrap model is not yet available to calculate the consequent correlated decays of pions of sundry charges. Here we simply assign charges statistically to the final pions without regard to the cluster from which they came. This includes effects from charge conservation ($n_{\pi^+} > n_{\pi^-}$) but no subtler effects.

2. PREDICTIONS

a) Multiplicity distributions

The two basic parameters λ and K_{max} introduced in Section 1.a are directly determined from the moments f_1 and f_2 of the multiplicity distributions. Thus, for a given mass m_B, the mean number of clusters is

$$\langle n_c \rangle = \lambda \ln (m_B^2) \tag{6}$$

while the observed particle yield is

$$f_1 = \langle n_\pi \rangle = \langle K \rangle \lambda \ln (m_B^2) \tag{7}$$

If the clusters are distributed in a Poisson fashion, we can easily show that

$$\begin{aligned} f_2 &= \langle n_\pi (n_\pi - 1) \rangle - \langle n_\pi \rangle^2 \\ &= \frac{\langle K(K-1) \rangle}{\langle K \rangle} \lambda \ln (m_B^2) \end{aligned} \tag{8}$$

f_2 is naturally positive in agreement with data [5].

These results are modified by both the integral over m_B presented by the proton distribution, and by energy momentum conservation effects which spoil the Poisson distribution for clusters produced from a given m_B. These are all included in our Monte Carlo program. For

$$\begin{aligned} \lambda &= 0.7 \\ K_{max} &= 8 \end{aligned} \tag{9}$$

We find results shown in Figs. 2a and 2b for f_1, γ_2 and γ_3. The latter are defined by

$$\gamma_2 = \langle (n-\langle n\rangle)^2\rangle / \langle n\rangle^2$$
$$\gamma_3 = \langle (n-\langle n\rangle)^3\rangle / \langle n\rangle^3 \qquad (10)$$

and are predicted to be constant if KNO scaling is true [14]. It is noteworthy that our model - for which KNO scaling has no significance - does exhibit it a as a transient phenomenon over the range 50 → 300 GeV/c, for which it has been tested.

It is worth noting here that the contribution of the Pomeron graph 1b gives a cross-section $\sigma^{(P)} \sim \log s$, a multiplicity $\langle n\rangle^{(P)} \sim \log s$ and an $f_2^{(P)} \sim (\log s)^2$. The total $\langle n\rangle$ and f_2 are given by

$$\langle n\rangle = a\langle n\rangle^{(P')} + b\langle n\rangle^{(P)}$$
$$f_2 = a f_2^{(P')} + b f_2^{(P)} + ab\left[\langle n\rangle^{(P')} - \langle n\rangle^{(P)}\right]^2 \qquad (11)$$

using "two-component" language. Here $a+b = 1$, $a = \sigma^{(p')}/\sigma$, $b = \sigma^{(P)}/\sigma$ so that at current energies, $\langle n\rangle$ has a term growing as $(\log s)^2$ and f_2 a $(\log s)^3$ component. As we indicated earlier, these results are quantitatively different from those in previous "two-component" treatments. Our model has the appealing feature that the same parameters λ and K_{max} control Pomeron and non-Pomeron terms. As pointed out by Frazer, Snider and Tan [13] this gives the asymptotic prediction $\langle n\rangle^{(P)} = \frac{1}{2}\langle n\rangle^{(p')}$. It can be tested experimentally by looking at multiplicity distribution of pions recoiling off a proton with, say $|x| > 0.9$. We expect a distribution with half the mean of the total sample. We find at the top of the ISR energy range, that the total multiplicity distribution develops a two-peaked structure corresponding to the two terms - P' and Pomeron in the model. Unfortunately, this double peak is smeared into one when the charged multiplicity distribution is examined. The main test then remains the x dependence of the multiplicity distribution mentioned above.

b) Momentum transfer distributions

The transverse momentum distribution is determined by the two parameters σ_1 and σ_2 introduced in Section 1.a. It is well known [15] that (except for one particle clusters !) the final pion transverse momentum is solely determined by σ_2 (given σ_1 is small, i.e., $\sigma_1 \lesssim \sigma_2$). We find a nice fit with the reasonable value $\sigma_2 = 230$ MeV/c. This gives the shape, for small p_T^2, of

$f(x,s,p_T^2)$ integrated over all x. Again the model, in quantitative agreement with experiment [16], predicts this distribution to be sharper for small x. Note that σ_2 not only determines the mean p_T^2 of the final π's but also the mass of the cluster decaying into a given number of pions [Eq. (3)]. An economy of parameters results.

c) Single particle inclusive distributions

Rapidity distributions at several energies are shown in Fig. 3a where we see scaling and the eventual appearance of a plateau at ISR energies *). The general shape and energy dependence (including rise at $y=0$ v. energy) is in good agreement with data [2),16),17)]. One failing is that experimentally [17)] the π^- distribution is sharper than the π^+ y distribution [i.e., $d\sigma/dy(\pi^-) < d\sigma/dy(\pi^+)$ in the fragmentation region]. This is easily understood in a Regge analysis, but cannot be reproduced with our present crude handling of charge. For this reason, we compare theory with the sum of π^+ and π^- distributions. Figure 3b shows $d\sigma/dy$ for various charged pion multiplicities. The sharpening of the y distribution for increasing multiplicity has been seen at ISR [4)] and NAL [16)]. A dip develops at $y=0$ for the low multiplicities as energy increases. This is a consequence of the increasing importance of Pomeron exchange.

These results can be understood analytically. The rapidity distribution of π's decaying from a single cluster is [18)]

$$d\,D_\pi/dy = \frac{1}{2\cosh^2(y-y_c)} \approx \frac{1}{\delta_0\sqrt{2\pi}} \exp\left\{-(y-y_c)^2/2\delta_0^2\right\} \qquad (12)$$

with $\delta_0 \simeq 0.9$.

Given a plateau in cluster rapidity, an integral over (12) implies a plateau in π rapidity. Now as each m_B gives a plateau, it is easy to see that for the P' graph 1c, the integral over m_B alters nothing. A single Pomeron graph 1b gives a cluster rapidity distribution

---

*) The energy at which a plateau appears is sensitive to small changes in parameters. For instance, a 20% increase in $\langle|x\,P'|\rangle$ would destroy the plateau at ISR energies.

$$d\sigma/dy^{(cluster)} \propto \log(\sqrt{s}) + y \qquad (13)$$

which peaks at $y = \log\sqrt{s}$. Upon adding the other Pomeron graph, we find a full plateau also for the net Pomeron contribution. The Monte Carlo program shows that energy momentum effects do not spoil this. The Pomeron graphs sum to give a plateau in y whose height rises like $\log(s)$ compared with the P' graphs. Such a plateau is of course not expected in the older two-component models where the Pomeron graphs only contribute to the edges of the rapidity plot [19].

d) Two-particle inclusive distributions

Our predictions for

$$R(y_1, y_2) = \frac{\sigma_{inel}\, d^2\sigma/dy_1 dy_2}{d\sigma/dy_1\, d\sigma/dy_2} - 1 \qquad (14)$$

are shown in Figs. 3c and 3d. We see that R is energy independent over the ISR range for $y_1 \approx 0$. For a y_1 that is outside the plateau, R rises with energy to its limiting form as a function of $y_1 - y_2$ only. These features all agree with data [3),4),20)], as does the rough shape and, in particular, the zero seen for $y_1 \approx 0$, $|y_2| \approx 3$.

Defining, as usual,

$$C(y_1, y_2) = \frac{1}{\sigma_{inel}^2} \frac{d\sigma}{dy_1} \frac{d\sigma}{dy_2} R(y_1, y_2) \qquad (15)$$

we can show that the contribution of Fig. 1c - the P' graph is

$$C^{(P')}(y_1, y_2) = F^{(P')} \frac{\langle K(K-1)\rangle}{\langle K\rangle} \times \frac{1}{2\delta_0\sqrt{\pi}} \exp\left\{-(y_1 - y_2)^2/4\delta_0^2\right\} \qquad (16)$$

with

$$F^{(P')} = 1/\sigma^{(P')}\, d\sigma^{(P')}/dy$$

Note that (16) gives a correlation length ≈ 2 units (defined as distance over which C falls to $1/e$ of its maximum value). It is an energy independent function of $|y_1-y_2|$ only. The Gaussian form in (16) is valid only for small $|y_1-y_2|$, where neglect of the pion mass implicit in (12) is valid *). On the other hand, the exponential form predicated by Mueller analysis [9] is correct only at large $|y_1-y_2|$. Thus there is no contradiction between the two approaches.

The correlation function for the Pomeron terms takes the form

$$C^{(P)}(y_1,y_2) = \tfrac{1}{2} F^{(P')^2}\left\{\tfrac{1}{2} - |y_1-y_2|/\log s\right\} + \frac{F^{(P')}}{2}\left\{1 - \frac{|y_1-y_2|}{\log s}\right\}\frac{\langle K(K-1)\rangle}{\langle K\rangle 2\delta_0\sqrt{\pi}}\exp\left\{\frac{-(y_1-y_2)^2}{4\delta_0^2}\right\} \quad (17)$$

This expression shows both short- and long-range pieces.

The net correlation function has, in addition to (16) and (17) a cross term

$$\frac{\sigma^{(P')}\sigma^{(P)}}{\sigma^2}\left\{\frac{1}{\sigma^{(P')}}\frac{d\sigma^{(P')}}{dy_1} - \frac{1}{\sigma^{(P)}}\frac{d\sigma^{(P)}}{dy_1}\right\} \times \left\{\frac{1}{\sigma^{(P')}}\frac{d\sigma^{(P')}}{dy_2} - \frac{1}{\sigma^{(P)}}\frac{d\sigma^{(P)}}{dy_2}\right\} \quad (18)$$

In some two-component work [19] $d\sigma^{(P)}/dy$ is assumed to be negligible at $y=0$, in which case the above term gives a considerable contribution at $y_1 \approx y_2 \approx 0$. In our case, because $\langle n^{(P)}\rangle \simeq \frac{1}{2}\langle n^{(P')}\rangle$, (18) is roughly 0.25 the values suggested previously [19]. Combining all effects of the Pomeron graph, (17) and (18), we find that our total "long range" contribution to $R(0,0)$ at ISR energies.is about 0.1, and is even smaller for large $|y_1-y_2|$.

The analytic calculation and Monte Carlo program both indicate that essentially all the correlation in the central region comes from the short-range component. The good agreement in Fig. 3a for charged correlations indicates that the same value $\langle K\rangle \simeq 4$, for pions per cluster decay [21], fits both f_2 and the correlation data.

Data [3] suggest a small constant positive value of R for large $|y_1-y_2|$. The analytic calculation is doubtful there, but the effect is not seen in our Monte Carlo calculation (cf., Fig. 3d). The small constant value is obtained

---

*) C. Hamer, private communication.

in two-component models. It is important to confirm this effect in the data, and to examine its sensitivity to technical assumptions in the theory.

It would be interesting to calculate $\pi^-\pi^-$ correlations in our model. This requires proper calculation of the cluster decay discussed in Section 1.d. The statistical bootstrap does have low-lying resonances (in particular $\pi^+\pi^-$ resonances ρ,f... and no $\pi^-\pi^-$ resonances) and so will predict a larger correlation for $\pi^+\pi^-$ than $\pi^-\pi^-$ - in agreement with experiment [20]. This direct channel calculation is dual to the Mueller approach to correlations, and it will be valuable to see if it is successful.

We are also examining other more complicated correlation data [22] reported from the ISR and so far find good agreement.

e) Dispersions

It was pointed out [18] recently that the dispersion of events provides a good measure of the extent of cluster formation in individual events. We define

$$\bar{y} = \sum_{i=1}^{\ell} y_i / \ell$$

$$\delta^1_{ch}(y) = \left\{ \frac{1}{\ell - 1} \sum_{i=1}^{\ell} (y_i - \bar{y})^2 \right\}^{1/2} \qquad (19)$$

where the sum runs over the ℓ particles obtained by removing the leading particle (farthest away in rapidity) from an $(\ell+1)$ charged particle final state. Our model, as in all multiperipheral models, predicts a logarithmic rise in $\delta^1_{ch}(y)$. The prediction is shown for two multiplicities in Fig. 2c. We calculated δ from this cluster model, from a simple multiperipheral production of π's not in clusters, and from the nova model at 300 GeV/c. Both the nova model and the cluster model agree qualitatively with the experimental dispersions at this energy [23]. [The Monte Carlo program indicates that these models would be distinguishable at 300 GeV/c if true rapidity and not the approximation $-\log(\tan\theta_{proj}/2)$ were used.] The nova model is ruled out at NAL and ISR energies by, say, the observed plateau in rapidity for low multiplicities, and so the cluster model is the only viable explanation. At $p_{lab} \leq 30$ GeV/c, where the nova model is particularly successful [6], our model and the nova model are very similar. At these energies, we can produce only one or two clusters, just as in the nova model. As s increases, the number of clusters grows in our model, rather than remaining fixed at one or two.

3. CONCLUSIONS

We have shown reasonable agreement between our model and experiment for essentially all the important attributes of multiparticle data at small transverse momenta. We feel this provides strong evidence for the input clustering and multiperipheral-like matrix element. Our results are much less sensitive to the treatment of diffraction (Pomeron exchange) and we can only claim consistency with and not evidence for the particular Pomeron model used. For instance, one can obtain just as good a fit to the multiplicity distributions with no Pomeron [$B=0$ in Eq. (5)]. The clusters and the integrals of proton x distributions provide sufficient distortion of the Poisson form to agree with experiment. Previous two-component models have perhaps been misleading in this respect.

Improvements to the model will come firstly from a better treatment of low mass m_B allowing meaningful calculations below 50 GeV/c. (Note at incident lab. momentum of 21 GeV/c we only have enough energy to produce one or two clusters.) Secondly, we must find the proper pion decay for a statistical bootstrap cluster which includes effects of charge and correlations between different pions. Again we can study $p\bar{p}$ and $K\bar{K}$ pair production - whose cross-sections are sensitive to mass dependence of produced clusters. Finally, similar models can be made for eN, νN and e^+e^- scattering and perhaps there too they will be successful.

Having in hand a simple framework which reproduces successfully the more striking features of NAL and ISR results, allows us to estimate the dynamical significance of other observations [22], in particular those not interpretable directly by fully inclusive (Mueller) analysis.

ACKNOWLEDGEMENTS

We thank C. Hamer for many discussions on the multiperipheral cluster model and A. Kryzwicki who originally suggested the possibility of treating nucleons in the way developed here. G.C.F. is grateful to the Theoretical Study Division, CERN, for hospitality during the period in which this work was completed.

REFERENCES

1) CERN-Holland-Lancaster-Manchester ISR Collaboration :
M.G. Albrow et al., Nuclear Phys. B54, 6 (1973).

2) British-Scandinavian ISR Collaboration :
B. Alper et al., paper submitted to XVI International Conference on High Energy Physics;
Saclay-Strasbourg ISR Collaboration :
M. Banner et al., Phys.Letters 41B, 547 (1972).

3) CERN-Hamburg-Vienna ISR Collaboration :
H. Dibon et al., Phys.Letters 44B, 313 (1973).

4) Pisa-Stony Brook ISR Collaboration :
G. Belletini, XVI International Conference on High Energy Physics, Chicago-Batavia, Vol.1, p.279 (1972).

5) Multiplicity data in pp collisions
13-28.5 GeV/c : E.L. Berger, B.Y. Oh, H. Ma and G.A. Smith (to be published).
50 and 69 GeV/c,: French-Soviet Mirabelle Collaboration, paper submitted to XVI International Conference on High Energy Physics.
100 GeV/c : J.W. Chapman et al., Phys.Rev.Letters 29, 1686 (1972).
200 GeV/c : G. Charlton et al., Phys.Rev.Letters 29, 515 (1972).
300 GeV/c : F.T. Dao et al., Phys.Rev.Letters 29, 1627 (1972).

6) E.L. Berger, M. Jacob and R. Slansky, Phys.Rev. D6, 2580 (1972).

7) G.H. Thomas and D. Sivers, Phys.Rev. D6, 1961 (1972).

8) A. Białas, K. Fialkowski and K. Zalewski, Nuclear Phys. B, to be published.
H. Harari and E. Rabinovici, Phys.Letters 43B, 49 (1973);
L. Van Hove, Phys.Letters 43B, 65 (1973);
J. Lach and E. Malamud, Phys.Letters 44B, 474 (1973);
P. Pirilä and S. Pokorski, Phys.Letters 43B, 502 (1973).

9) A. Mueller, Phys.Rev. D2, 2963 (1970).

10) C.J. Hamer, Brookhaven preprint (1972).

11) C.J. Hamer and R. Peierls, Brookhaven preprint (1973).

12) R. Hagedorn, Nuovo Cimento Suppl. 3, 147 (1965);
S. Frautschi, Phys.Rev. D3, 2821 (1971).

13) A. Capella and M.-S. Chen, SLAC-PUB-1252;
W.R. Frazer, D.R. Snider and C.-I. Tan, San Diego preprint UCSD-10P10-127;
G.F. Chew, Berkeley preprints LBL-1556 and LBL-1701;
D. Amati, L. Caneschi and M. Ciafaloni, CERN report TH.1676 (1973).

14) Z. Koba, H.B. Nielsen and P. Olesen, Nuclear Phys. B40, 317 (1972).

15) E. Yen and E.L. Berger, Phys.Rev.Letters 24, 695 (1970).

16) The "sea-gull" effect ($\langle p_T \rangle$ small for small x) is well known at low energies. For pp at 200 GeV/c, see
Y. Cho et al., report NAL-PUB-73/26-EXP, ANL/HEP.7316.

17) Michigan-Rochester Collaboration 103 GeV/c NAL data as presented in Fig. 5 of J. Whitmore, International Conference on High Energy Particle Collisions, Vanderbilt (1973).

18) E.L. Berger, G.C. Fox and A. Krzywicki, Phys.Letters 43B, 132 (1973).

19) P. Pirilä and S. Pokorski, loc. cit.

20) ANL-NAL Collaboration :
J. Whitmore, loc. cit.

21) In a multifireball model developed by Hasegawa, the value of four particles for fireball is also found.
Y. Fujimoto and S. Hayakawa, in Handbuch der Physik, Vol. XLVI/2, p.115 (Springer Verlag, 1967).

22) M.G. Albrow et al., Phys.Letters 44B, 207 and 518 (1973).

23) F.T. Dao et al., NAL-PUB-73/2E-EXP, May 1973.

FIGURE CAPTIONS

Figure 1 : a) Multiperipheral production of clusters by exchanges denoted "π" for definiteness.

b) Pomeron exchange contribution to inclusive proton production.

c) Regge exchange contribution to proton production, typified by P' exchange.

Figure 2 : a) Calculated mean number of negative tracks $\langle n_- \rangle$ in proton-proton collisions versus lab. momentum. Data are from Ref. 5).

b) Multiplicity distribution moments γ_2 and γ_3 [Eq. (10)] for negative tracks. Data points are derived from Ref. 5)

c) Central value and standard deviation of dispersion δ^1 of individual events in rapidity [cf., Ref. 18) and Eq. (19)]. Values are shown for charged multiplicity $n_{ch} = 10$ and 20.

Figure 3 : a) Single pion inclusive rapidity distribution $\sigma_{inel}^{-1} d\sigma/dy$ versus y_{lab} for 28.5, 205, 500 and 1500 GeV/c. Theoretical curves are normalized absolutely and summed over all charges. Data at 100 GeV/c [Ref. 17)] are $1.5 \times [d\sigma/dy(\pi^+) + d\sigma/dy(\pi^-)]/\sigma$.

b) Rapidity distribution $\sigma_n^{-1} d\sigma_n/dy$ for intervals of charged pion multiplicity n are given at 500 GeV/c. Shown also for comparison is the 1500 GeV/c result for the selection $1 \leq n \leq 5$.

c) Normalized inclusive charged particle correlation function $R(y_1, y_2)$, defined in the text [Eq. (14)], plotted versus y_2 for selections $|y_1| \leq 0.25$. Preliminary data are from Ref. 4) at 500 GeV/c while predictions are given at 500 and 1500 GeV/c. Note the data use the approximation $y \approx \log(\tan\theta/2)$ but the Monte Carlo program indicated this has little effect on distributions.

d) as c), but for $1.7 \leq y_1 \leq 2.7$.

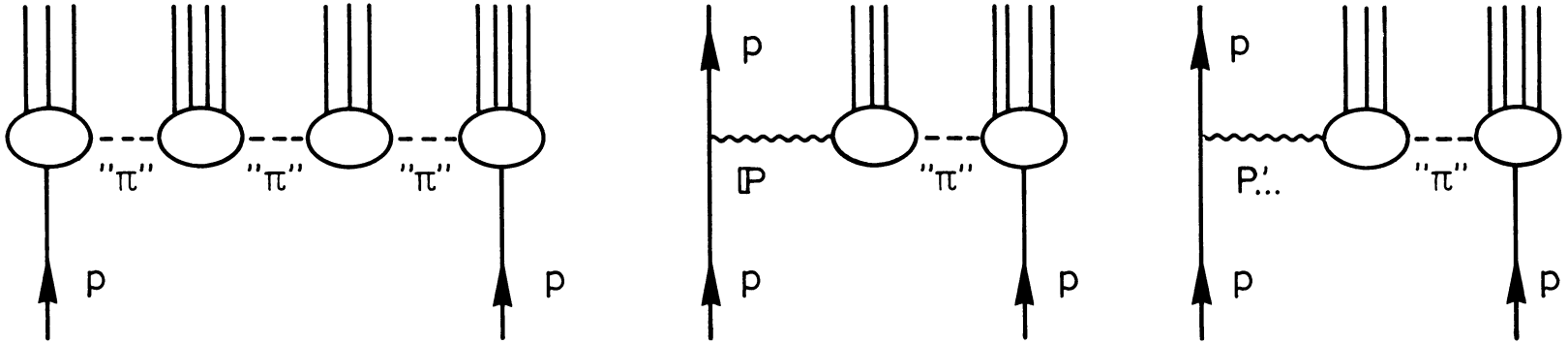

FIG. 1

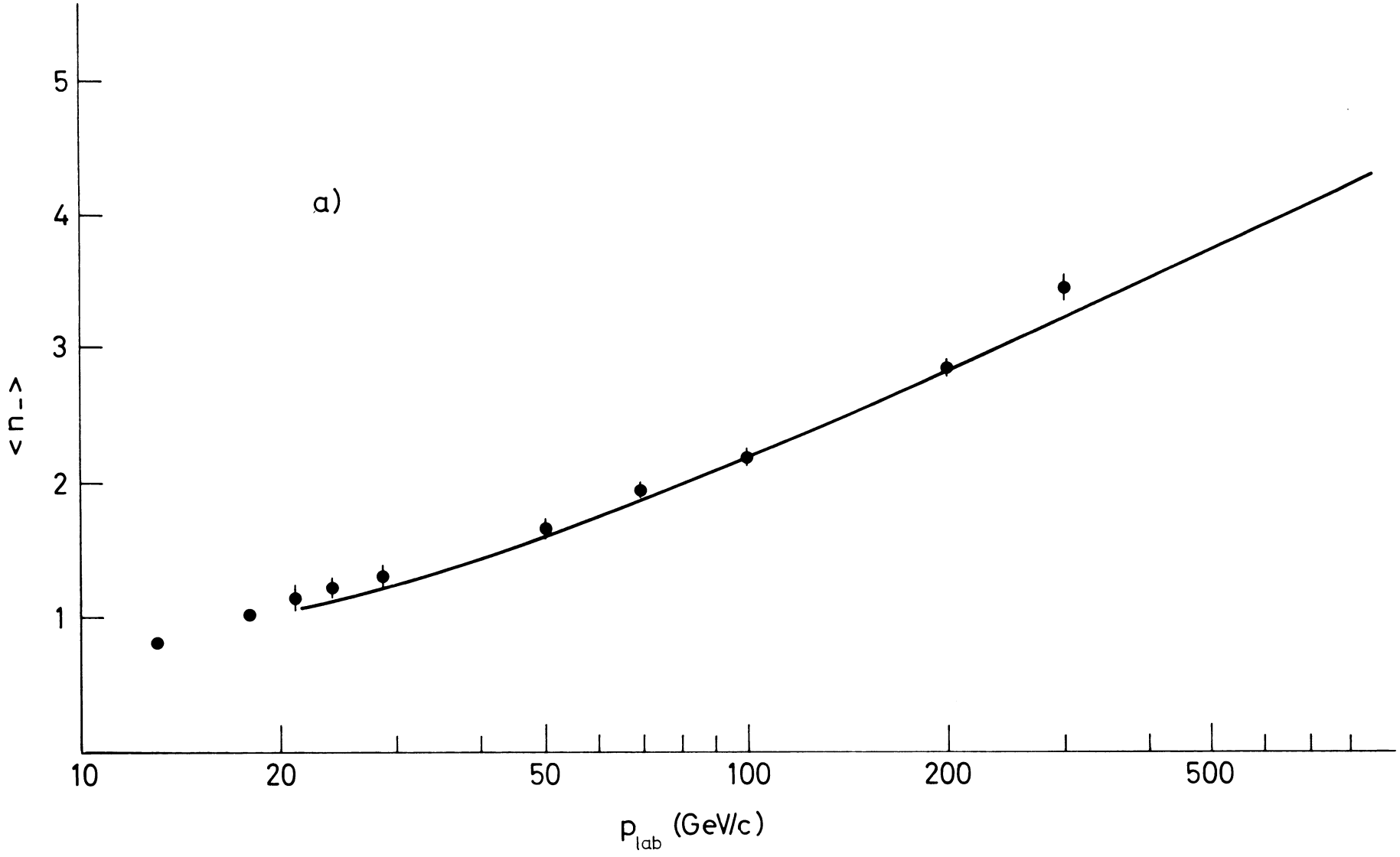

FIG. 2

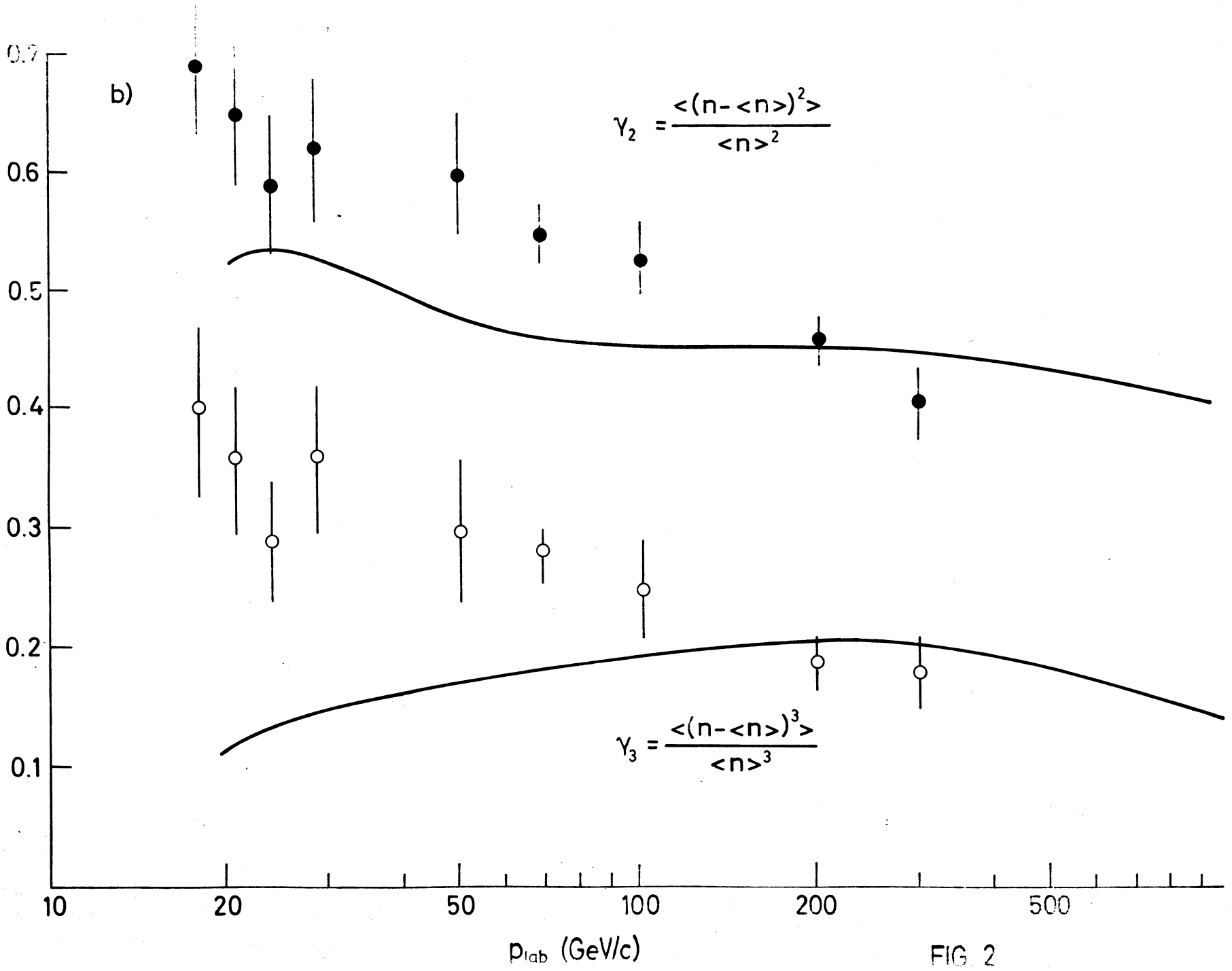
b)
$\gamma_2 = \frac{\langle (n-\langle n\rangle)^2\rangle}{\langle n\rangle^2}$
$\gamma_3 = \frac{\langle (n-\langle n\rangle)^3\rangle}{\langle n\rangle^3}$
0.7
0.6
0.5
0.4
0.3
0.2
0.1
10
20
50
100
200
500
p_{lab} (GeV/c)

FIG 2

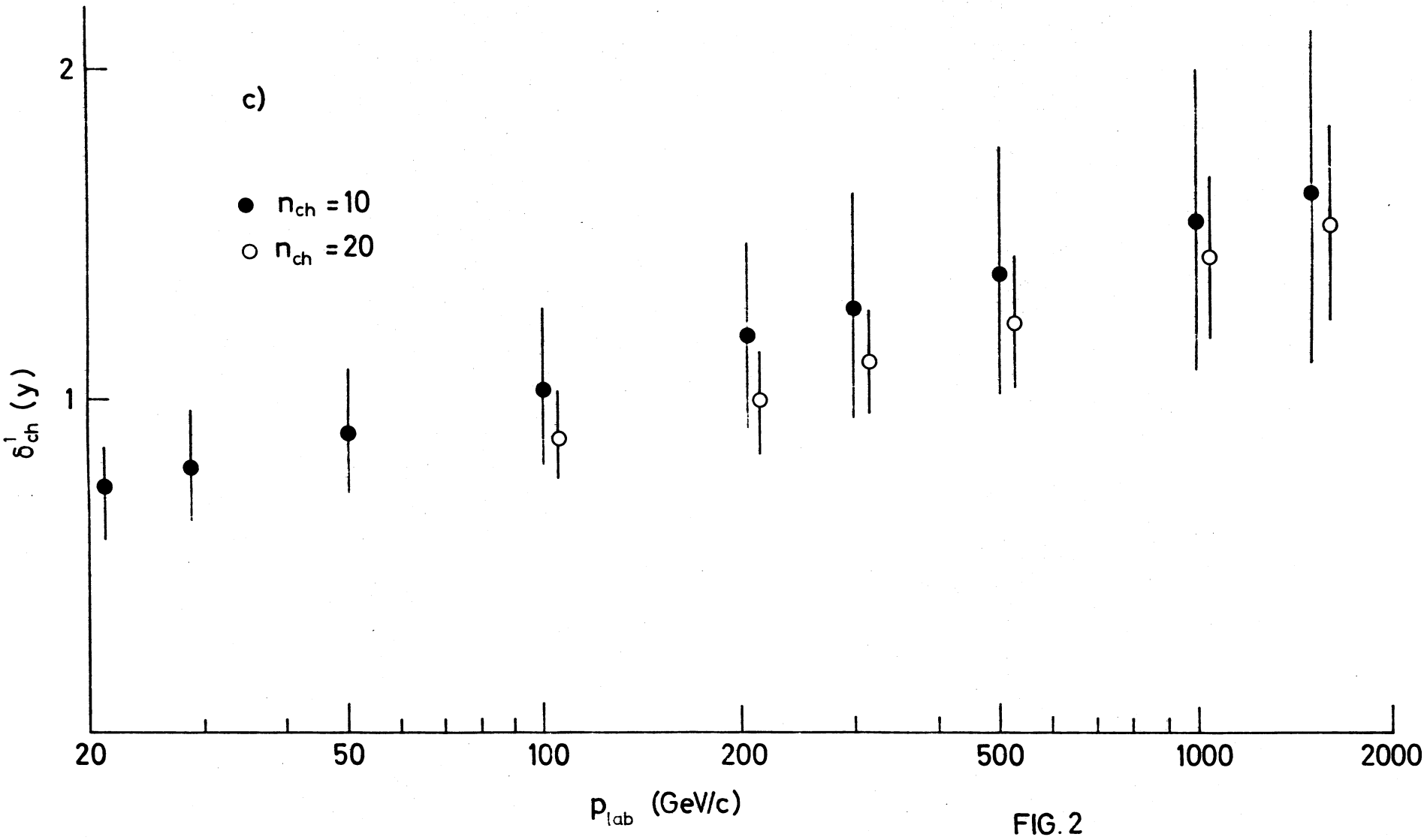
c)
● $n_{ch} = 10$
○ $n_{ch} = 20$
δ^1_{ch} (y)
2
1
20
50
100
200
500
1000
2000
p_{lab} (GeV/c)

FIG. 2

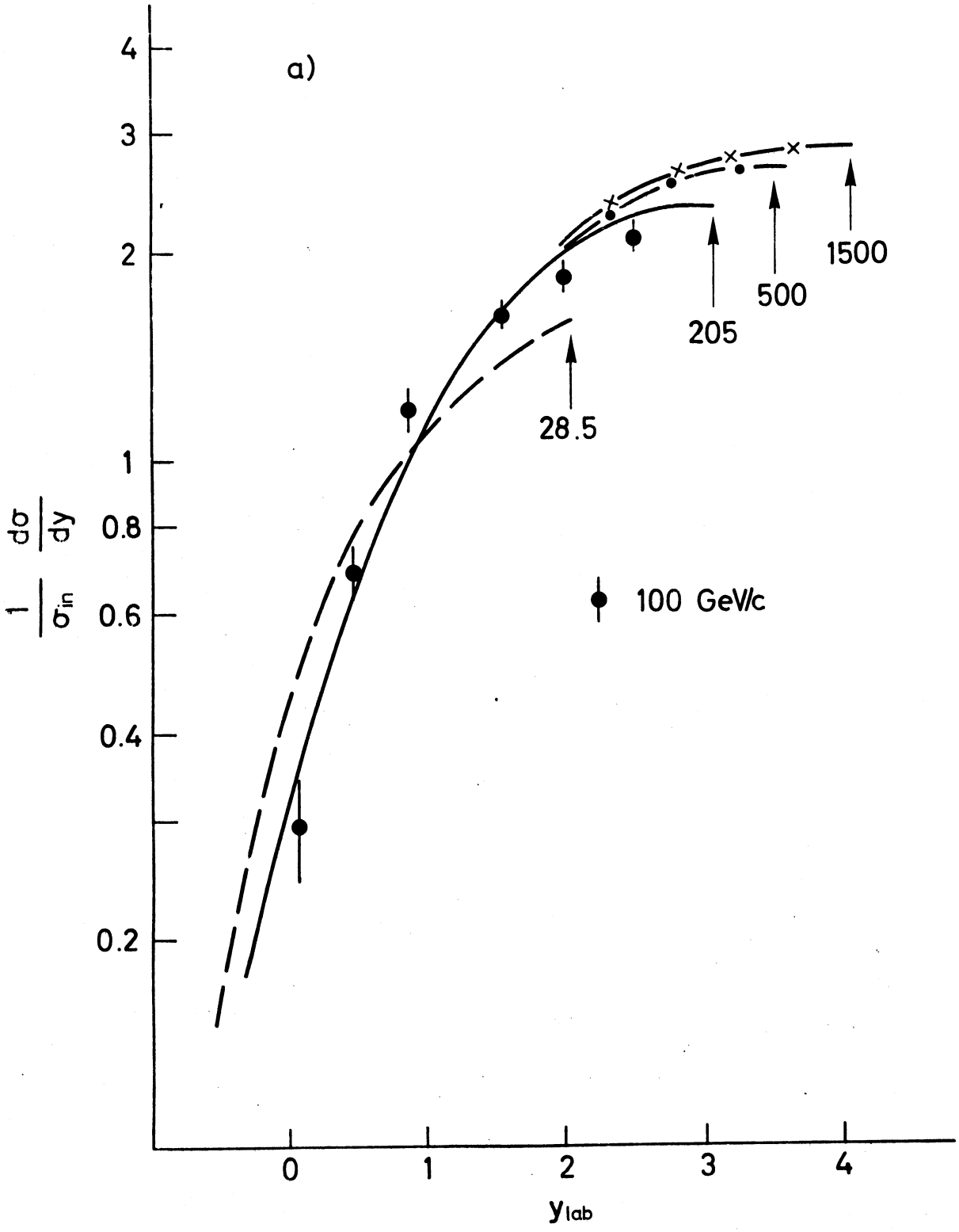
a)
4
3
2
1
0.8
0.6
0.4
0.2
0
1
2
3
4
$\frac{1}{\sigma_{in}} \frac{d\sigma}{dy}$
y_{lab}
28.5
205
500
1500
100 GeV/c

FIG. 3

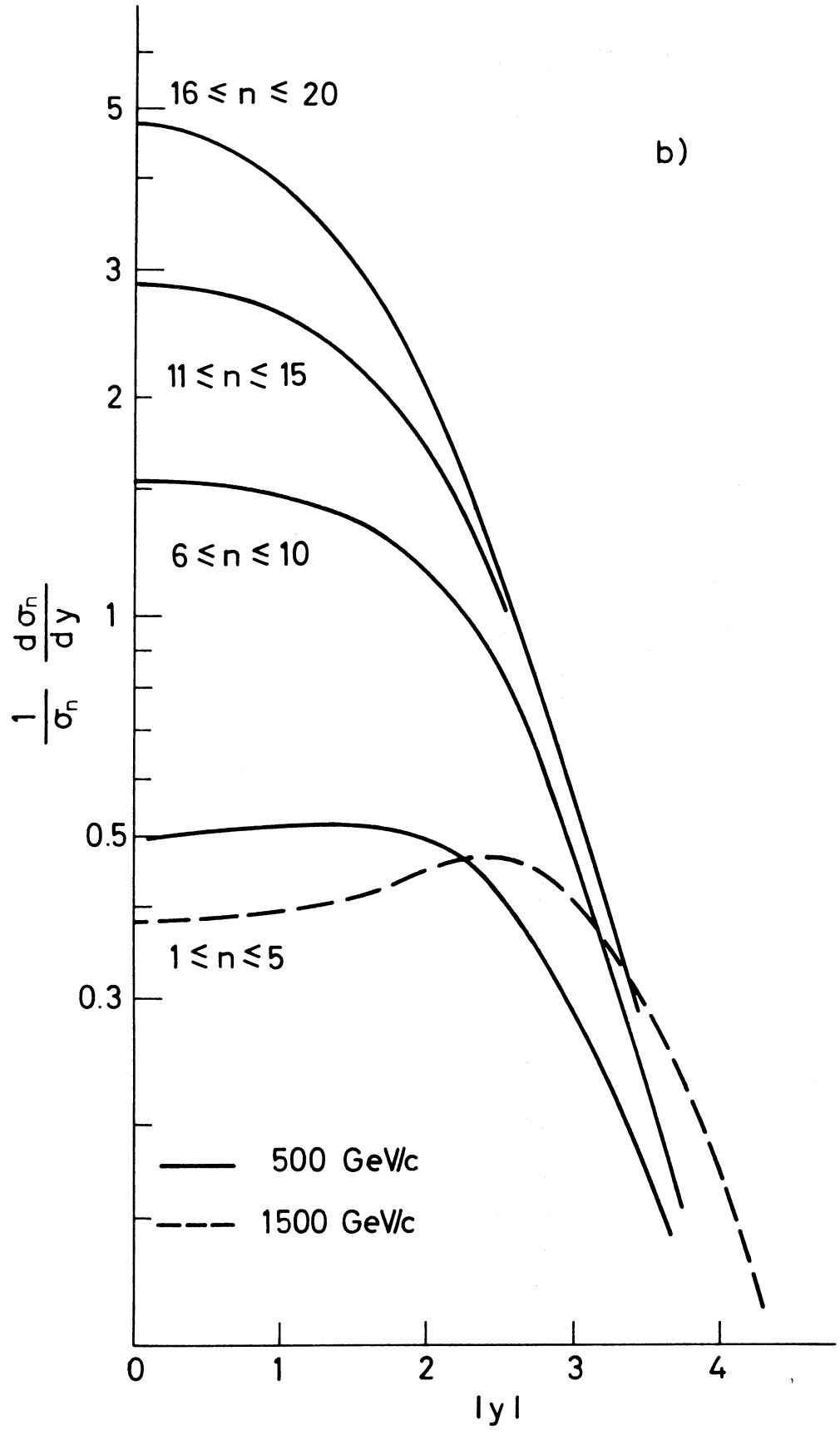
b)
16 ≤ n ≤ 20
11 ≤ n ≤ 15
6 ≤ n ≤ 10
1 ≤ n ≤ 5
500 GeV/c
1500 GeV/c
$\frac{1}{\sigma_n}\frac{d\sigma_n}{dy}$
5
3
2
1
0.5
0.3
0
1
2
3
4
|y|

FIG. 3

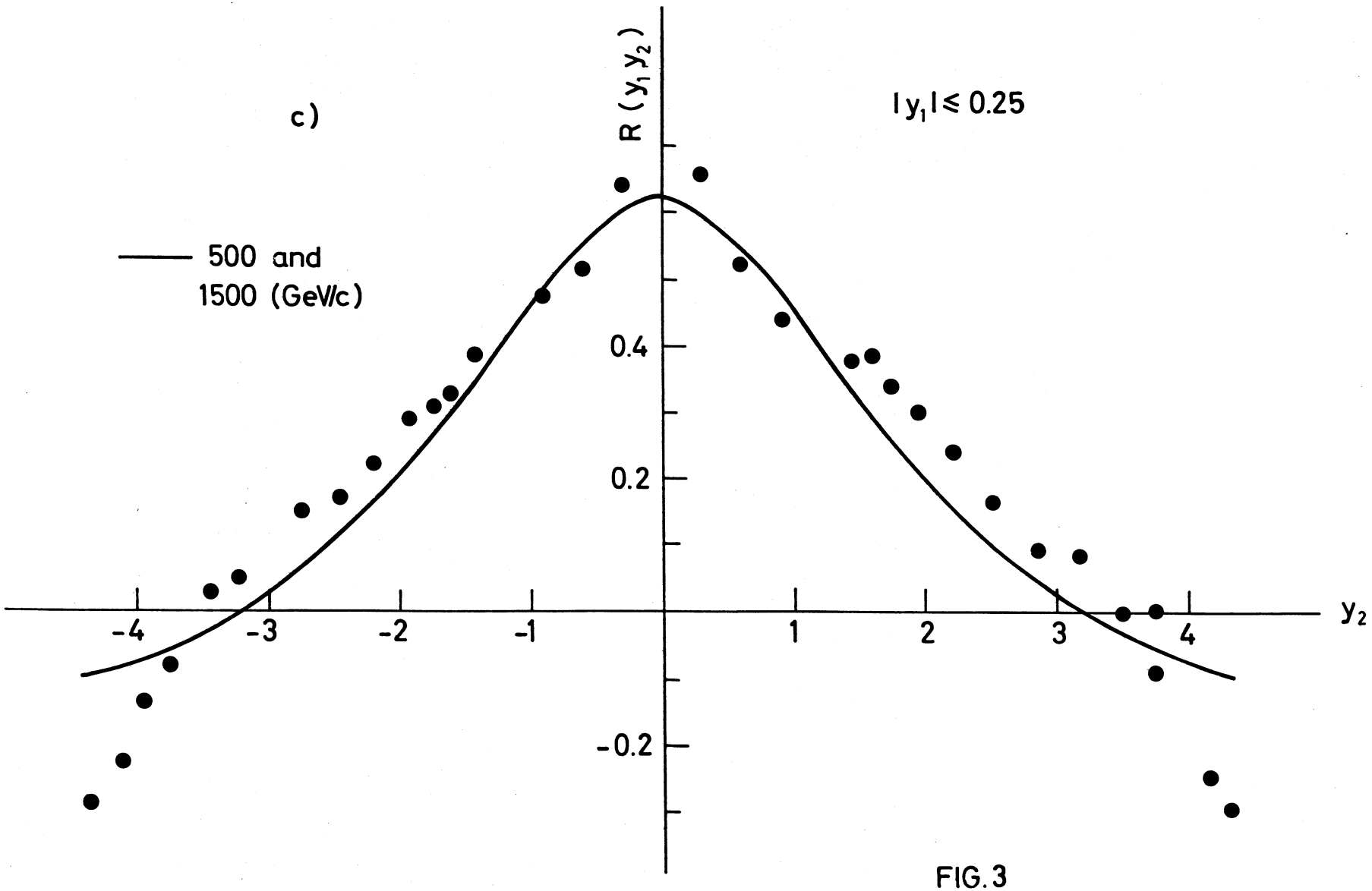

FIG. 3

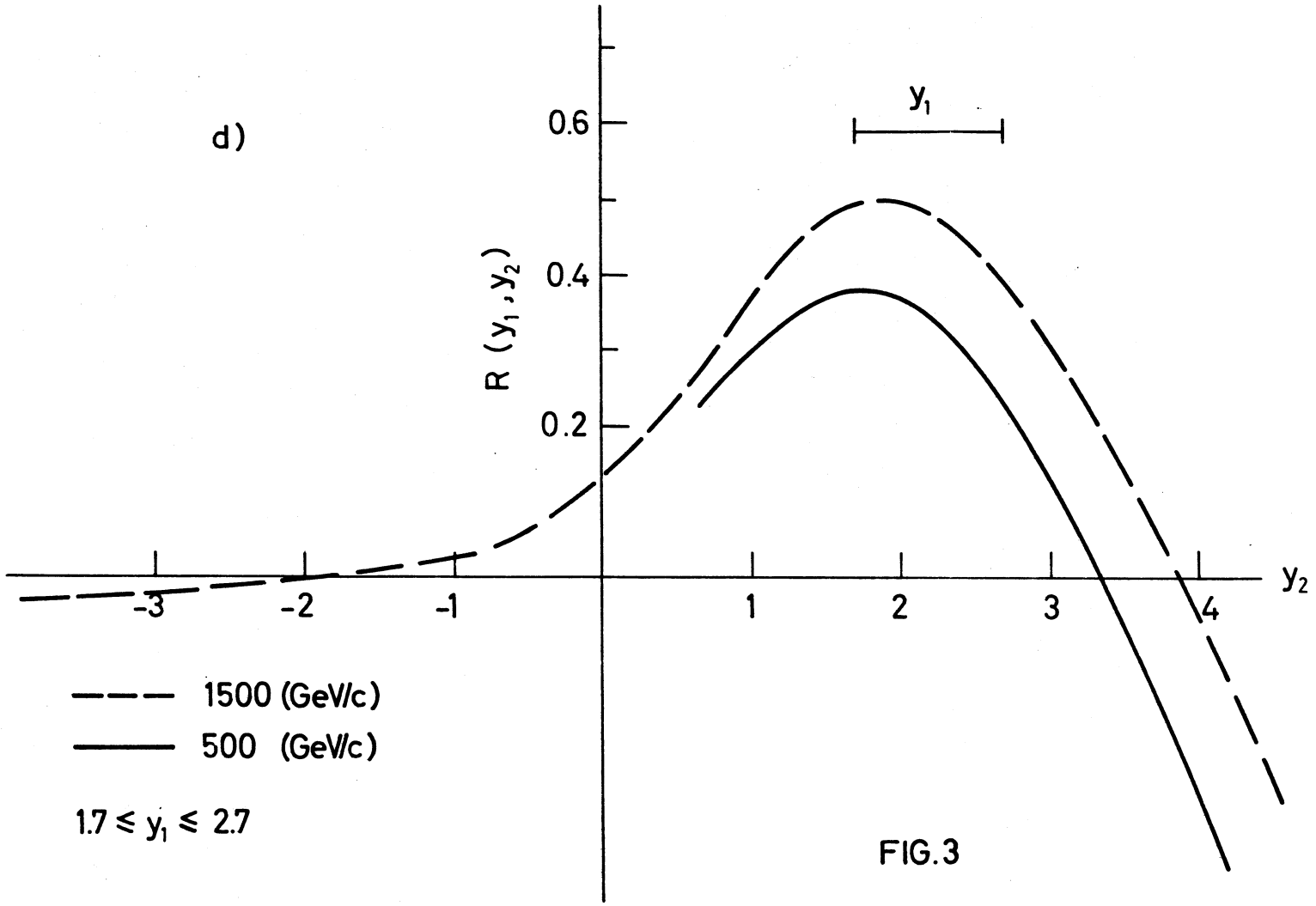
d)
0.6
0.4
0.2
$R(y_1, y_2)$
y_1
y_2
-3
-2
-1
1
2
3
4
1500 (GeV/c)
500 (GeV/c)
$1.7 \leq y_1 \leq 2.7$

FIG.3